Academic Journal of Science and Technology
ISSN: 2771-3032 | Vol. 2, No. 2, 2022

Synthesis of Water-Soluble Chitosan and Study of Water-Soluble Chitosan Nanospheres

Yifeng Hu[1], Hongxia Li[1, *]

[1] School of Pharmacy, Jiangsu University, Zhenjiang 212013, PR China

[*] **Corresponding author**: Hongxia Li, Email: lihongxia@ujs.edu.cn

Abstract: Objective N-octyl-N '- (2-carboxycyclohexanecarbonyl) -chitosan derivative (OCCC) was successfully synthesized. The analysis of the chitosan derivative by infrared spectroscopy, nuclear magnetic resonance spectroscopy and the like was used to verify whether the synthesis was successful. To construct and characterize chitosan nanoparticles with bovine serum albumin as the model drug. The transmission electron microscopy (TEM), encapsulation efficiency, drug loading and in vitro release of the constructed nanoparticles were investigated. Methods OCCC-BSA-NPs were prepared by ion cross-linking method, and we investigate the release of nanoparticles in vitro. Results The optimum conditions were OCCC:TPP concentration = 10:1, ρ (TPP) = 0.8mg / ml, Time = 40min. Under these conditions, the maximum encapsulation efficiency and drug loading were 91.12% and 4.11%, respectively. The drug- loaded nanoparticles were placed in pH = 7.4 PBS, and the release rate reached about 80% at 10h, and reached 90% at 48h, which achieved the effect of sustained release.

Keywords: Synthesize, Chitosan, BSA, Nanoparticles, Release, Encapsulation efficiency, Drug loading.

1. Introduction

Chitosan [α (1→4) 2-amino 2-deoxy β-D-glucan], a cationic polysaccharide obtained from the deacetylation of chitin, has received wide attention as a pharmaceutical excipient because of its unique properties such as biocompatibility, biodegradability, low-immunogenicity and non-toxicity[1,2]. Studies[3-5] have shown that chitosan has excellent biocompatibility and biodegradability, and safe and non-toxic, which is known as one of the most promising drug delivery materials. Chitosan as a drug carrier can play a role in controlling drug release, prolonging efficacy, reducing toxic side effect, improving the stability of hydrophobic drugs, changing the route of administration and so on, and enhancing the targeting ability of the preparation[6,7]. Chitosan chemical structure shown in Figure 1[8].

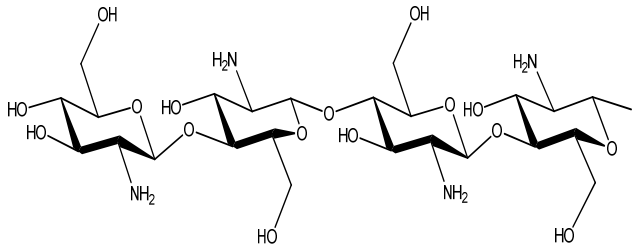

Figure 1. Chitosan chemical structure[8]

Despite of its superiority as a biomaterial, chitosan is not fully soluble in water and then soluble in acidic solution. Aqueous solubility of chitosan only in acidic solution because of its rigid crystalline structure and the deacetylation which limits its application to bioactive agents such as gene delivery carriers, peptide carriers, and drug carriers[9-11]. Water-soluble chitosan is easily soluble in neutral aqueous solution. Its advantage is ease of modification, useful as gene or peptide drug carriers. Therefore, water-soluble chitosan and functional property have been developing for pharmaceutical and new drug candidate.

Bodmeier[12] first proposed the preparation of chitosan microspheres by ion cross-linking. This method uses polyanion as a physical crosslinking agent, combined with the positively charged amino group after protonation of the chitosan molecular chain, reversibly, intermolecular or intermolecularly crosslinking mainly by electrostatic action, and then gelatinizing the chitosan to form spherical particles. The chemical structure shown in Figure 2 [13] .

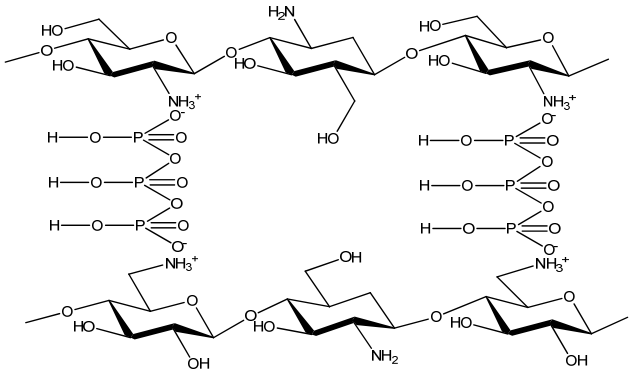

Figure 2. Chemical structure of microspheres formed by the cross - linking reaction between chitosan and sodium tripolyphosphate[13]

Taking this into account, the purpose of the current study was to investigate water-soluble chitosan as a carrier system for protein delivery and some factors affecting drug delivery. In this study, an amphiphilic N-octyl-N'- (2-carboxycyclohexanecarbonyl) -chitosan (OCCC) was designed and synthesized to solve the problem that chitosan is insoluble in water. Then BSA was used as model drug, chitosan derivatives OCCC as carrier material and sodium tripolyphosphate as crosslinking agent. The BSA-loaded chitosan nanoparticles(BSA-OCCC-NPs) were prepared by ion-crosslinking method, and their formulations were

optimized and characterized.

2. Materials and Methods

Materials

Chitosan (degree of deacetylation >90%, molecular weight 600,000 Da, Jinan Hyderabel Marine Biology Co., Ltd.), Sodium tripolyphosphate (TPP, Shanghai Kechang Fine Chemicals Co., Ltd.), Bovine serum albumin (BSA, Sigma), Coomassie brilliant blue G250 (Sigma Chemical Co). Hexahydrophthalic anhydride ($C_8H_{10}O_3$, Sigma). Dimethyl sulfoxide(DMSO, Sigma). The other reagents are of analytical grade. Transmission electron microscopy (Hitachi H-600), UV-Vis spectrophotometer (Beijing General Analysis-T6), FD-1B-50 type freeze-drying machine (Beijing Bo Kang Kang Experimental Instrument Co., Ltd.), TGL-16B high-speed desktop centrifuge (Anke), PB-10 pH meter (Sartorius), CP225D Electronic Analytical Balance (Sartorius), 79-1-type magnetic stirrer (Guohua enterprises), ZRS-8G intelligent dissolution tester (days of the day Technology Co., Ltd.).

Method

2.1. Synthesis of Water-soluble chitosan(OCCC)

We weighed chitosan (CS, 4mg, 70kDa) in anhydrous methanol (120ml) with mechanical stirring in a 30 °C water bath. Octanal(11.3ml) was added slowly, and then keep it warm for 8h. Join in KBH_4 (3g, 56mmol) partially, with room temperature reduction reaction 24 h. After the reaction, 1 mol/L NaOH was used to adjust the pH to 7, and then the sample is filtered. Firstly, wash the sample with water twicely. Secondly, wash the sample with methanol four times. Finally, obtain pale yellow powder after drying is OC (3.8 g, 84.4 %).

2.1.1. Preparation of N-octyl chitosan (OC)[14]

We weighed chitosan (CS, 4mg, 70kDa) in anhydrous methanol (120ml) with mechanical stirring in a 30 °C water bath. Octanal(11.3ml) was added slowly, and then keep it warm for 8h. Join in KBH_4 (3g, 56mmol) partially, with room temperature reduction reaction 24 h. After the reaction, 1 mol/L NaOH was used to adjust the pH to 7, and then the sample is filtered. Firstly, wash the sample with water twicely. Secondly, wash the sample with methanol four times. Finally, obtain pale yellow powder after drying is OC (3.8 g, 84.4 %).

2.1.2. Preparation of N-octyl-N'- (2-carboxycyclohexylcarbonyl) -chitosan derivative (OCCC)[15]

We weighed N-octyl chitosan(OC, 0.5g, 0.68mmol) in Dimethyl sulfoxide(DMSO, 25ml) with swelling 2h. With stirring at room temperature, hexahydrophthalic anhydride(0.6g, 2 mmol) was added in a three-necked flask. The temperature rosed to 80 °C and then reacted for 24h. 55 mL of water was added to the reaction solution, and then the pH of the reaction solution was then adjusted to 10 with 20% NaOH in an ice-water bath. The filtrate was dialyzed against a semi-permeable membrane (cut-off molecular weight 10000) for 5 days after the sample extraction. White flocculent solid was obtained after lyophilization(0.45g, 86.5%).

2.2. Characterization of the Synthesized Product

2.2.1. Characterization of Infrared Spectroscopy (FTIR)

Potassium bromide (KBr) tabletting method: The medicine and KBr by 1: 100 ratio were grinding and mixing. Then keep it tabletting.

2.2.2. Characterization of Nuclear Magnetic Resonance Spectroscopy (^{1}H-NMR)

The samples were dissolved in deuterated heavy water (D_2O) as solvent and tetramethylsilane (TMS) as internal standard. The samples were characterized by ^{1}H-NMR.

2.3. Preparation of Water - Soluble Chitosan Blank Nanoparticles

We weighed the right amount of OCCC dissolved in double distilled water, to formulate into a certain concentration of chitosan solution whose pH adjusted to 4-6. Then we filtered with 0.45μm filter. We weighed the right amount of sodium tripolyphosphate dissolved in distilled water whose pH adjusted to 7-8. Then we filtered with 0.22μm filter. Weigh 5ml OCCC solution in a round bottom flask and keep it continue magnetic stirring. Slowly drop 1ml sodium tripolyphosphate solution with dropping rate of 20-40 drops per minute. Stop dropping, and then continue magnetic stirring for a certain period of time.

2.4. Characterization of OCCC-BSA nanoparticles

2.4.1. Transmission Electron Microscopy (TEM) Observe the Morphology of OCCC-BSA Nanoparticles

The OCCC-BSA nanoparticles were prepared by the prescription process and diluted 100 times with distilled water. In the copper mesh point, dry after 2.0% phosphotungstic acid solution for 10min, dry under TEM observed under the morphology of nanoparticles.

2.4.2. Zeta Potential and Particle Size Analysis of OCCC-BSA Nanoparticles

Weigh a certain amount of OCCC-BSA nanoparticle lyophilized powder, which dissolved in pH = 7.4 phosphate buffer solution (PBS), and then ultrasound 3min. With 0.45μm filter membrane impurity removal, determine Particle Size Distribution and Surface Potential by Dynamic Light Scattering Method (DLS).

2.5. Determination of Entrapment Efficiency and Drug Loading

Measure 5ml OCCC solution and add an equal volume of BSA solution, with keep it continue magnetic stirring and slowly dropping 1ml TPP. Steady dripping was continued for a certain time and then the BSA was encapsulated in the nanoparticles. The encapsulation efficiency was calculated by the BSA chitosan nanoparticle dispersion at 4°C, 15000 r / min, 20min, and the free BSA content measured by bradford method. The centrifuged sample was washed with double distilled water(DDW) and then freeze dried to calculate the drug loading. BSA entrapment efficiency and drug loading were calculated according to indicated below[17]:

Entrapment efficiency% = [(the total amount of drug - the amount of free drug) / the total amount of drug] × 100%

Drug loading%= [(the total amount of drug - the amount of free drug)/ the quality of nanoparticles] × 100%

2.6. Optimization Design of Orthogonal Experimental Design

In order to optimize the preparation process, according to the results of the pre-test and the relevant literature, four factors, which are most influential to the properties of the nanoparticles, were selected as the object of study. Three levels were selected for each factor. According to the orthogonal design principle, Orthogonal test table $L_9(3^4)$ for the experiment.. The test factors and levels are shown in Table 1.

Table 1. Orthogonal factors and levels (n=3)

Factor	OCCC concentration: TPP concentration (mg/ml)	TPP concentration (mg/ml)	BSA concentration (mg/ml)	Time (min)
Level 1	10: 1	0.6	0.8	30
Level 2	12: 1	0.8	1.0	40
Level 3	14: 1	1.0	1.2	50

2.6.1. Evaluation of Orthogonal Experiment Design Data

The optimal preparation process of chitosan nanoparticles was optimized by the encapsulation efficiency and drug loading of drug-loaded nanoparticles. The encapsulation efficiency and drug loading were determined according to "2.5" in this paper.

2.7. Release of OCCC-BSA Nanoparticles In Vitro

According to the Chinese Pharmacopoeia 2010 edition of the two appendix release degree determination in the first law of the determination [18]. The release of nanoparticles was determined by two release media, respectively. Release medium 1: pH = 1.2 hydrochloric acid solution; Release medium two: pH = 7.4 phosphate buffer solution. The temperature and rotation were adjusted to 37◦C and 90 rpm, respectively. At predetermined time of 1, 2, 3, 4, 6, 8, 16, 24 and 48 hour, 5 mL of sample was removed and ultracentrifuged at 15,000 r/min for 30 minutes, and 5 mL of the supernatant were replaced by fresh medium. The percentage of cumulative release of protein was calculated by measuring the protein content of bradford method.

3. Results and Discussion

3.1. Preparation and Characterization of N-Octyl-N'-(2-Carboxycyclohexanecarbonyl) - chitosan Derivatives (OCCC)

3.1.1. Synthesis of N-octyl - N'- (2-carboxycyclohexanecarbonyl) –chitosan

Synthetic route shown in Figure 4.

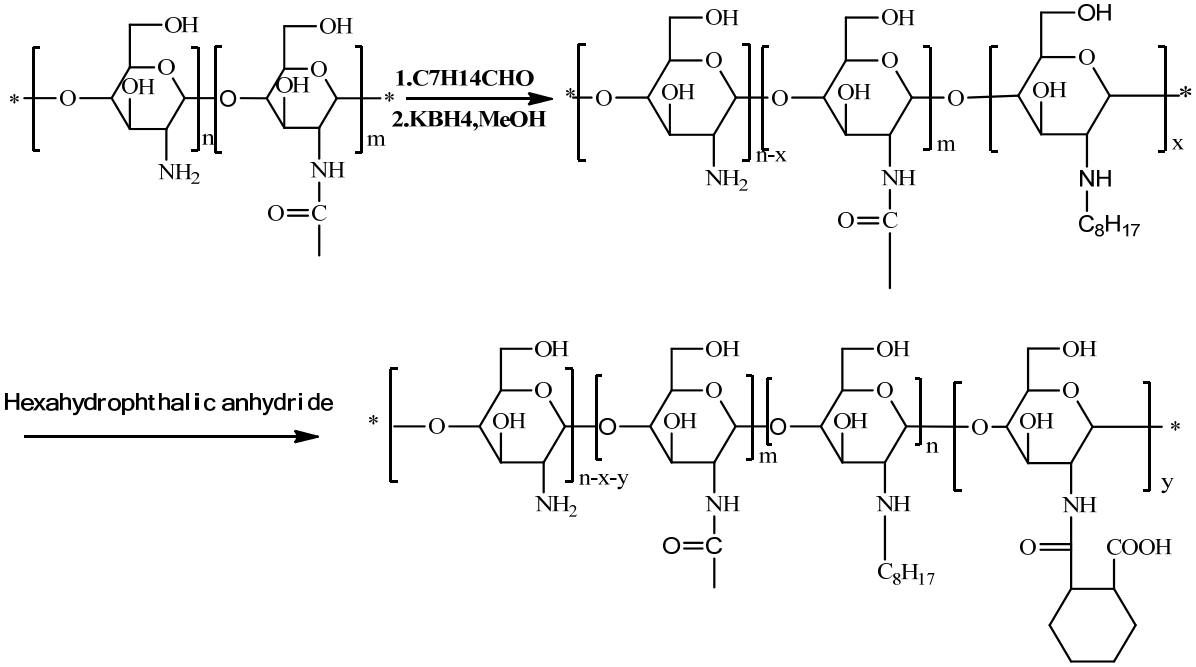

Figure 4. Synthesis of N-octyl-N'-(2-carboxycyclohexanecarbonyl)-chitosan

3.1.2. Infrared spectroscopy (FTIR) characterization

Infrared spectrum shown in Figure 5. As the infrared spectrum shown in the figure, 1564 cm^{-1} is the C = O stretching vibration of the secondary amide. Chitosan derivative (OCCC) increases the -CH_2- stretching vibration of alkanes relative to chitosan 2927 cm^{-1}. 2358cm^{-1} is probably stretching vibration peak of -CH- , but also increase the amide bond , and it is probably at 1600-1800 cm^{-1}.

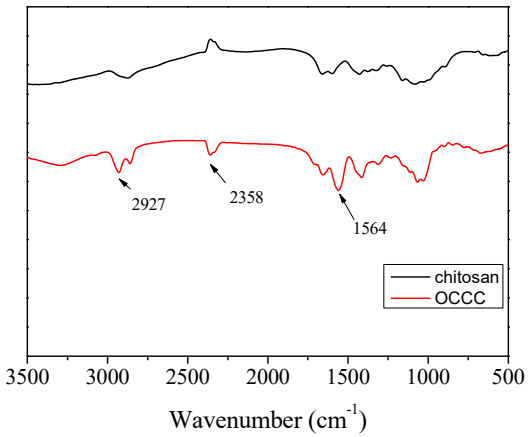

Figure 5. IR spectra of chitosan and OCCC

3.1.3. Nuclear Magnetic Resonance (^{1}H-NMR) Characterization

Nuclear magnetic resonance spectrum shown in Figure 6.

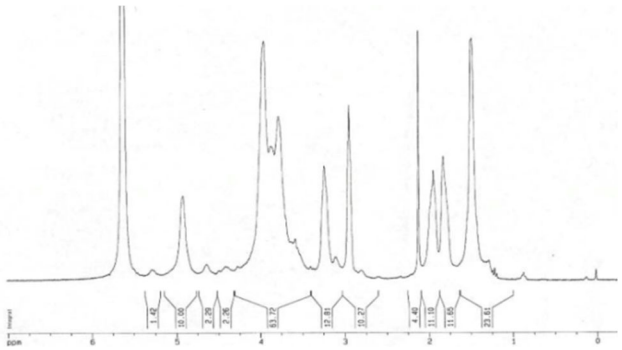

Figure 6. ^{1}H-NMR (D_2O) spectra of OCCC

In the picture of ^{1}H-NMR spectra of OCCC, δ (ppm) 1.5 is the hydrogen of octyl group. The signal peak of δ (ppm) 1.4-1.9 belongs to hydrogen on cyclohexane, and the signal peak of δ (ppm) 2-5 belongs to the shell poly Sugar skeleton peak. 5.6 is the solvent peak.

3.1.3 Nuclear Magnetic Resonance Carbon Spectroscopy (^{13}C-NMR) Characterization

Figure 3.4 is the ^{13}C-NMR of the target OCCC, 57 (C2), 62 (C6), 72 (C3), 77 (C5), 79 (C4) and 99 (C1) are the carbon signals of chitosan, 180 and 163 is a new occurrence that belongs to the carbonyl carbon signal, and the strong signal peaks appearing in the newly appearing 44, 28 and 25 are attributed to the carbon of cyclohexane and long chain alkanes.

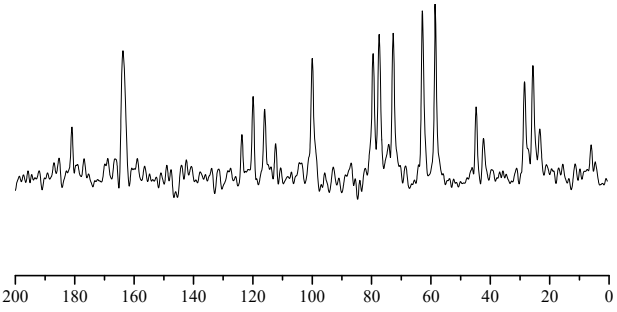

Figure 7. ^{13}C-NMR (D_2O) spectra of OCCC

3.1.4. Physical properties of N-octyl-N'-(2-carboxycyclohexaneformyl)-chitosan derivative (OCCC)

From the powder X-ray diffraction pattern of OC and OCCC (Fig.8), it is seen that sharper diffraction peaks appear at 12° and 20°, respectively, which belong to the I and II crystallographic bands, respectively. After the modification, the crystal diffraction peak of the OCCC at 2θ=12° disappeared, and the diffraction peak at 2θ=22° also became weak and became a broad peak. The results show that after the introduction of a hydrophilic group on chitosan, the ability to form a hydrogen bond is reduced, and a part of the crystalline form is converted into an amorphous form.

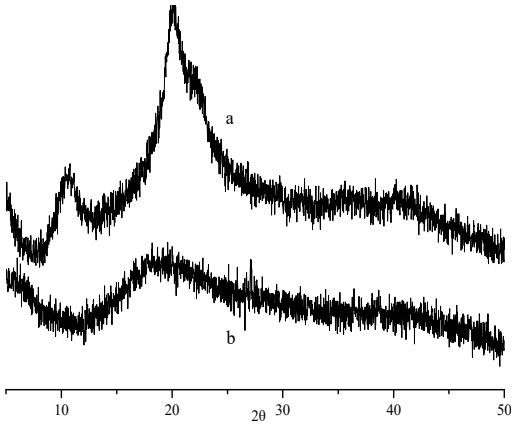

Figure 8. XRD patterns of (a) OC and (b) OCCC

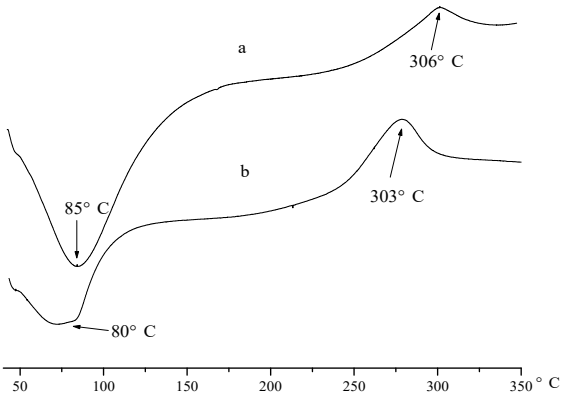

Figure 9. DSC thermograms of (a) OC and (b) OCCC

The DSC chart of N-octyl chitosan and its derivative OCCC is shown in Figure 9.

N-octyl chitosan and water-soluble chitosan OCCC showed a solvent volatilization endothermic peak at 80-85°C, thermal decomposition occurred at about 300°C, and N-octyl chitosan degradation peak appeared at 306°C, the thermal degradation peak of the water-soluble chitosan derivative OCCC appeared at 301°C, indicating that the crystallization ability decreased from order to disorder due to the introduction of octyl and amide substituents on the chitosan amino group.

3.2. Preparation and Characterization of Water - Soluble Chitosan OCCC-BSA nanoparticles

3.2.1. Characterization of Water Soluble Chitosan OCCC nanoparticles

The prepared nanoparticles were characterized by transmission electron microscopy (TEM) (Figure 10). It can be seen from the photos that the particle size of the nanoparticles is relatively uniform, which the shape is round or similar to round, and no agglomeration occurs. The particle size is about 278.56nm. Figure b is a photograph of chitosan

nanoparticles coated with BSA. It can be seen from the photos of the drug-loaded nanoparticles which successfully wrapped BSA, and the particle size of about 355.83nm. After drug loading nanoparticles have increased the size, and the edge of the shape is less regular. This is due to the presence of a large number of hydrophilic nanoparticles on the surface, part of the BSA adsorbed on the surface.

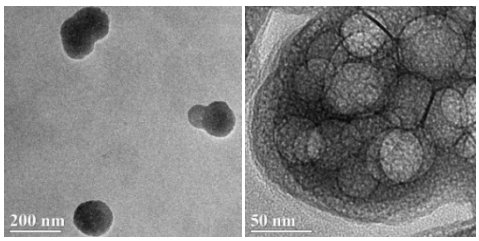

Figure 10. TEM micrograph of OCCC nanoparticles(a.OCCC-NPs; b. OCCC-BSA-NPs) ρ (CS) =1.6mg/ml, ρ (TPP) =0.8mg/ml, ρ (BSA)=1.2mg/ml

3.3. Determination of sustained release effect of OCCC-BSA nanoparticles

3.3.1. Single Factor Test Results[19,20] (n=3)

Effects of OCCC concentration on entrapment efficiency and drug loading

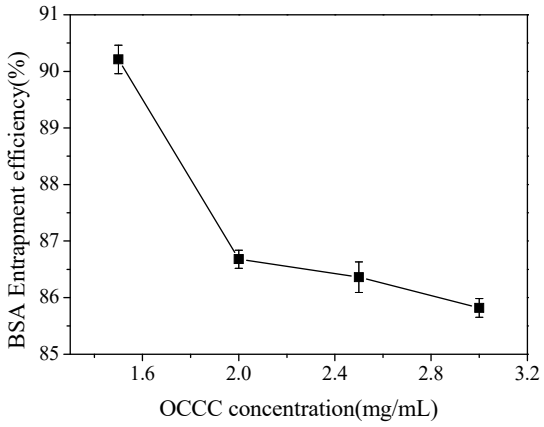

Figure 11. Effect of OCCC concentration on BSA entrapment efficiency

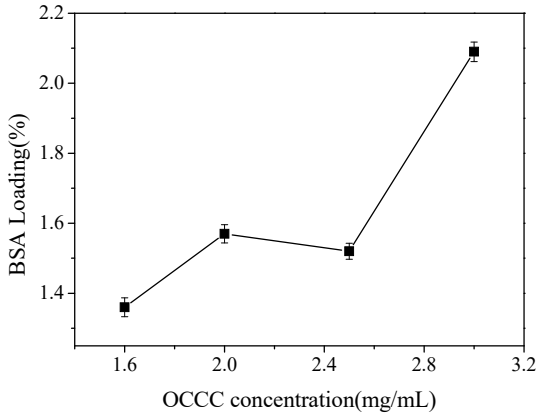

Figure12. Effect of OCCC concentration on BSA loading

Figure.11 and 12 were investigated different concentrations of OCCC on the encapsulation efficiency and drug loading of BSA. As seen from Figure 6, the entrapment efficiency decreases with increasing initial concentration of water-soluble chitosan, which is different from chitosan nanoparticles. Because water-soluble chitosan is a gel medium after it is dissolved in water, and the highly viscous nature of the gel medium hindered the encapsulation of BSA on chitosan nanoparticles. Lower concentrations of OCCC have lower adhesion, which promote encapsulation of BSA and gelation between chitosan and TPP. Figure.12 shows that as the concentration of OCCC increases, the drug loading increases. The reason of it is that with the concentration of added OCCC increases, the amount of drug-loaded nanoparticles increases and the amount of drug entrapped increases cause the increase of the drug loading.

Effects of crosslinking agent on entrapment efficiency and drug loading

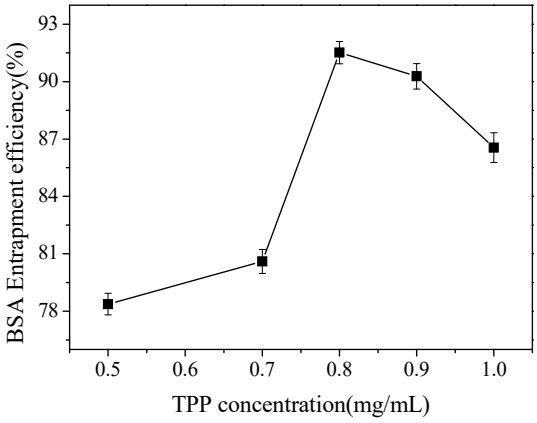

Figure 13. Effect of TPP concentration on BSA entrapment efficiency

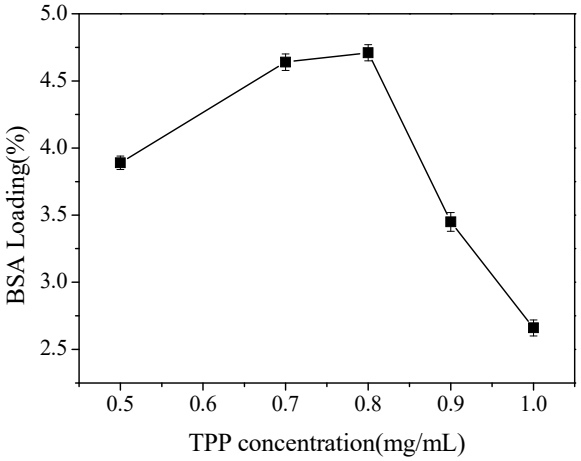

Figure 14. Effect of TPP concentration on BSA loading

Figure.13 and 14, respectively, is effects of the crosslinking agent sodium tripolyphosphate solution(TPP) on BSA encapsulation efficiency and drug loading. It can be seen from Figures.13 and 14 that when the TPP concentration is less than 0.8mg / ml, both the entrapment efficiency and drug loading increase as the TPP concentration increases. Increasing the concentration of crosslinkers increases the density of the nanoparticles, which in turn increases the encapsulation of BSA. Compared with chitosan as a carrier, the amount of crosslinking agent added is reduced, reducing the damage to the drug.

Effects of BSA initial concentration on entrapment efficiency and drug loading

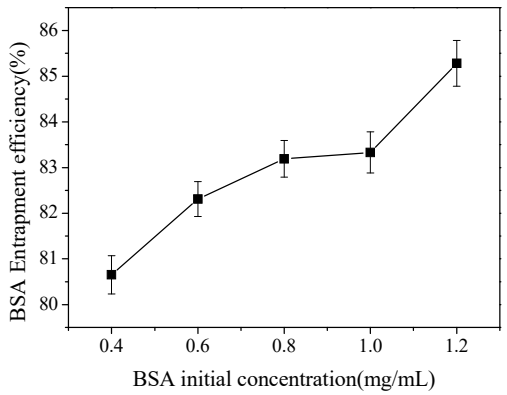

Figure 15. Effect of BSA initial concentration on BSA entrapment efficiency

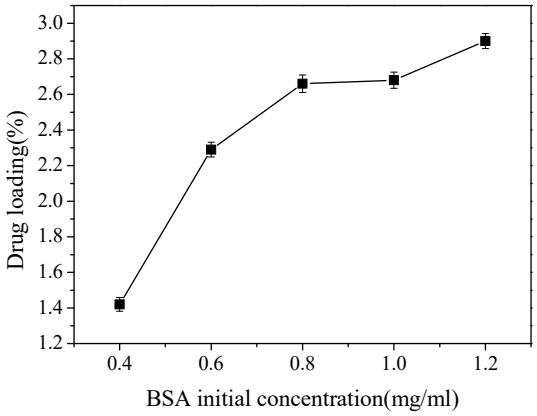

Figure 16. Effect of BSA initial concentration on BSA loading

Figure.15 and 16, respectively, is effect Effects of BSA initial concentration on entrapment efficiency and drug loading. As shown figures, as the amount of initial BSA input increases, the amount of protein added increases much more than the amount of encapsulation and drug loading, so the encapsulation efficiency and drug loading overall show an upward trend. As the concentration of BSA added increased, the mass of nanoparticles encapsulated drug also increased, leading to the increase of drug loading.

Effect of crosslinking time on entrapment efficiency and drug loading.

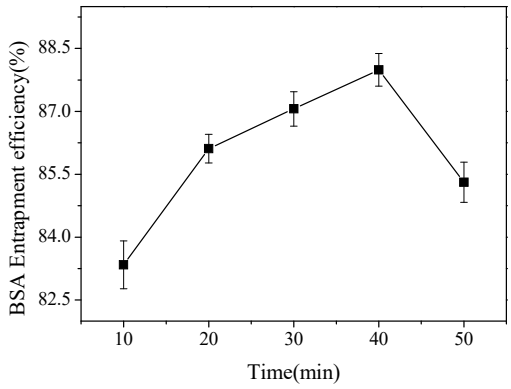

Figure 17. Effect of Time on BSA entrapment efficiency

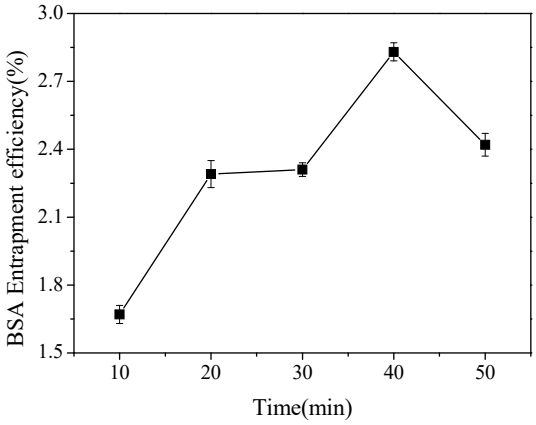

Figure 18. Effect of Time on BSA loading

Figure.17 and 18, respectively, is effect Effects of crosslinking time on entrapment efficiency and drug loading. It can be seen from the figures that when the crosslinking time is 40 min, the entrapment efficiency and drug loading of the nanoparticles are the largest.

3.3.2. Orthogonal Test Design Results

The repetition of three batches of nanoparticles were prepared and the test results were evaluated by taking the average drug loading and entrapment efficiency. The results of the orthogonal test are shown in Table 3.

From the range to determine the order of primary and secondary factors: A> C> B> D. It can be seen, $A_1C_2B_2D_2$ better than other combinations.

Table 2. Investigation on the optimal conditions for the formulation of OCCC-NPs by orthogonal design (L_9 (34))

factor	A	B	C	D	Entrapment efficiency (%)	Drug loading (%)	Overall rating: Overall rating
1	1	1	1	1	89.43±1.32	3.19±0.08	52.69
2	1	2	2	2	90.12±1.04	3.11±0.09	52.84
3	1	3	3	3	91.16±2.01	3.18±0.06	53.53
4	2	1	2	3	87.78±1.46	3.22±0.07	51.94
5	2	2	3	1	88.51±1.31	3.65±0.09	53.38
6	2	3	1	2	84.15±1.22	3.32±0.08	50.38
7	3	1	3	2	79.92±2.31	5.14±0.09	52.81
8	3	2	1	3	76.57±1.72	4.27±0.07	48.96
9	3	3	2	1	77.51±1.43	4.11±0.09	49.03
K1	53.020	51.480	50.677	51.700			
K2	51.900	52.727	51.270	52.010			
K3	50.267	50.980	53.240	51.477			
R	5.752	1.688	5.402	0.215			

Entrapment efficiency: The highest EEmax of the nine groups was 100 points and EEmin was 0. The remaining groups were calculated according to the following formula: Entrapment efficiency = 100-100 × (EEmax - Entrapment efficiency) / (EEmax - EEmin).
Drug loading: The highest DLmax of the nine groups was 100 points and DLmin was 0 points, and the remaining groups were calculated according to the following formula: Drug loading = 100-100 × (DLmax - Drug loading) / (DLmax - DLmin).
Overall rating: Overall rating = (Entrapment efficiency + Drug loading × 5) / 2

3.3.3. OCCC-BSA Nanoparticles in Vitro

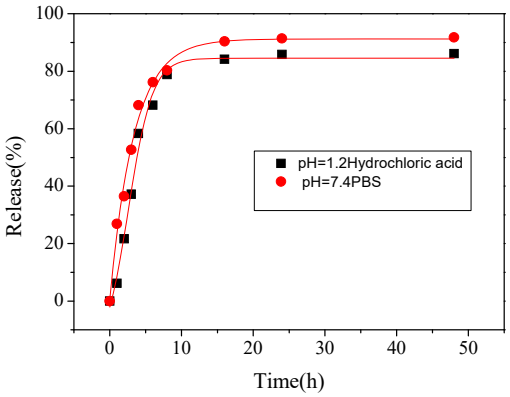

Figure 19. BSA release in different release media ρ (CS)= 1.6mg/ml, ρ (TPP)=0.8mg/ml, ρ (BSA)=1.2mg/ml

According to the orthogonal experiment analysis, the optimum conditions were selected to prepare nanoparticles. Figure 14 shows the release profiles of drug-loaded nanoparticles under optimal conditions in pH = 1.2 HCl solution and pH = 7.4 PBS, respectively. It can be seen from the figure that the release of drug-loaded nanoparticles in pH = 7.4 PBS is higher than that in hydrochloric acid solution, which proves that drug-loaded nanoparticles are more suitable for release in body fluids. In addition, the release of the nanoparticles reaches about 80% at 10 h, and reaches 90% at 48h, which achieves the sustained release effect.

4. Conclusion

The amphiphilic pH-sensitive chitosan graft copolymer N-octyl-N '- (2-carboxycyclohexanecarbonyl) -chitosan was successfully synthesized in this experiment. Its structure The synthesized target is expected to be a new type of pH-sensitive polymeric micelle material to solubilize insoluble drug. N-octyl-N '- (2-carboxycyclohexanecarbonyl) -chitosan nanoparticles were prepared by ion cross-linking in this paper and characterized by transmission electron microscopy (TEM). On the basis of this, the encapsulation and sustained release effect of the nanoparticles on BSA were studied. The results showed that the entrapment efficiency and drug loading of chitosan nanoparticles increased with the initial concentration of chitosan. Beginning with the increase of BSA initial concentration, the encapsulation efficiency and drug loadings also will increase. Therefore, CS have a potential carrier in a controlled drug delivery system for protein drugs. This chitosan derivative has a potential carrier in a controlled drug delivery system for protein drugs.

References

[1] Simon CW R, Hanno VJ K, Ruth D. Potential of low molecular mass chitosan as a DNA delivery system: biocompatibility, body distribution and ability to complex and protect DNA [J]. International Journal of Pharmaceutics, 1999, 178(2): 231-243.

[2] Choi C, Nam J P, Nah, J W. Recombinant Human TGF-beta 1 Protein [J] Chem. 2016, 33, 1-10.

[3] Croisier F, Jerome C. Chitosan-based biomaterials for tissue engineering[J] . European Polymer Journal, 2013, 49(4) : 780-792.

[4] Dash M, Chiellini F, Ottenbrite R M, et al. Chitisan- a versatilese semi-synthetic polymerin biomedical applocations [J]. Progress in polymer Science, 2011, 36(8) : 981- 1014.

[5] Jayakumar R, Menon D, Manzoor K, et al. Biomedical applications of chitin and chitosan based nanomaterials- a short review [J] . Carbohydrate Polymers, 2010, 82(2) : 227- 232.

[6] Sannan T, Kurita K, Iwakura Y. Studies on chitin: effect of deacetylation on solubility [J]. Chem. 1976, 177:3589-3600.

[7] Seo H, Shoji A, Itoh Y, et al. Antibacterial fiber blended with chitosan [J]. Chitin World, 1994: 623-631.

[8] Anitha A, Sowmya S, Kumar P T S, et al. Chitin and chitosan in selected biomedical applications [J]. Progress in Polymer Science, 2014, 39(9): 1644-1667.

[9] Lee D, Zhang WD, Shirley A, et a1. Thiolated chitosan/DNA nanocomplexes exhibit enhanced and sustained gene delivery [J]. Pharm Res, 2006, 24(1): 157-167.

[10] Li HY, Birchall J. Chitosan-modified dry powder form ulationsforpulmonary gene delivery [J]. Pharm Res, 2006, 23(5) : 941-951.

[11] Jin H, Kim TH, Hwang SK, et a1. Aerosol delivery of urocanicacid modifled chitosan/programmed cell death 4 complex regulatedapoptosis, cell cycle, and angiogenesis in lungs of Kras null mice [J]. Mol Cancer Ther, 2006, 5(4): 1041-1049.

[12] Bodmeier, R., Chen, H., Paeratakul, O., 1989. A Novel Approach to the Oral Delivery of Micro- or Nanoparticles. Pharm. Res. 6, 413–7.

[13] ZouXue, Zhao Xiaowen, Ye Lin, et al. Preparation and drug release behavior of pH- responsive bovine serum albumin-loaded chitosan microspheres [J]. Journal of Industrial and Engineering Chemistry, 2014.

[14] OH K T, KIM D, YOU H H, et al. pH-Sensitive properties of surface charge-switched multifunctional polymeric micelle[J]. Int J Pharm, 2009, 376(1/2): 134-140.

[15] ZHANG C, DING Y, YU L L, et al. Polymeric micelle systems of hydroxycamptothecin based on amphiphilic N-alkyl-N-trimethyl chitosan derivatives [J]. Colloids Surf B Biointerfaces, 2007, 55(2):192-199.